JOURNAL OF OPTOELECTRONICS AND ADVANCED MATERIALS Vol. 24, No. 3-4, March – April 2022, p. 162-167

Research studies on kerf quality of cutting single crystal diamond with water-jet guided laser

X. ZHANG[#], Q. WEI[#], H.-X. WANG[*]
Institute of Wide Band Gap Semiconductors, School of Electronics and Information Engineering, Xi'an Jiaotong University, Xi'an 710049, China
[#]*These authors contributed equally to this study and share the first authorship*

Water-jet guided lasers are an advanced technology which offers precision and efficiency for processing single crystal diamonds (SCD). In this paper, the slicing of high-pressure-high-temperature (HPHT) SCD samples via water-jet guided laser and conventional dry-laser were performed respectively. It is analyzed by SEM and Raman methods that a "V-shape" has turned out in a cross section and a graphite layer on kerf surface by conventional dry-laser slicing, but a smoothly flat cross-section without diamond structure change on kerf surface was achieved by water-jet guided laser slicing. The relationship between laser parameters and cutting depth were tested, in which cutting depth is linear growth with increasing laser power and cutting depth was decreased in general with increasing cutting speed but low cutting speed which causes bad kerf quality. The optimal quality of kerf surface was obtained when the cutting speed and laser power are set as 8mm/s and 11 W, respectively, and the corresponding minimum heat-affect zone (HAZ) is 3.983 μm. After laser power increased to 11.8 W, the SCD sample could be sliced completely with 8.306 μm of HAZ.

(Received September 17, 2020; accepted April 8, 2022)

Keywords: Water-jet guided laser, Single crystal diamond (SCD), Heat affect zone (HAZ)

1. Introduction

Diamond has long been held as a precious material in the jewelry industry and is a well-known semiconductor worldwide. In the last twenty years, a significant revolution has taken place in much of the diamond-manufacturing industry [1]. Because of chemical vapor deposition (CVD) and high-pressure-high-temperature (HPHT) techniques have lead diamonds to be made possible to be used to form thick films. Diamonds have 5.5 ev large bandgap, more than 10 $MV \cdot cm^{-1}$ theoretical electric breakdown field, high carrier mobilities, the highest thermal conductivity (2200 W/K·m) in the world, $0.8x10^{-6}$/K thermal expansion coefficient and effective resistance etc [2-6]. Therefore, it has been a promising material that has gained lots of attention for scientist, due to its unique properties in electronic devices and high-power and high-frequency technical areas. A good technique of machining diamonds has become an important skill in order to achieve a desirable artificial diamond thin film.

Lasers have had a wide variety of applications in many areas, such as medicine, metrology, manufacturing industry, optical communication etc [7] that is all because of its characters of high power, less divergence angle, short light pulse, better monochromaticity and continuously tunable spectrum output [8-9]. Of specific interest to manufactures, being able to use laser technology in diamond cutting in order to increase productivity and quality maximization has become the most desirable achievement. The traditional way of cutting a diamond is using dry-laser technology, which leads to a significant material sacrifice, a thick heat-affected zone (HAZ), a big amount of molten residues, V-shape cutting kerf and last but not least a short working distance. The water-jet guided laser processing is a breakthrough machining technology, which has quite a lot of benefit over the conversional laser slicing process and has overcome most of its drawbacks and not require focal optics. As a candidate of SCD sample slicing technology in this research, the water-jet guided laser technology is great because of its efficiency, precision without blurs, less heat and few pollution etc [10]. The laser of that technology comes from a high pressure micro-meter-thin de-ionized pure water by pump. Apart from guiding the laser beam as a "water fiber" between air and water, the water jet also works as a spontaneous cooler and washes away molten pieces and reduces fumes during machining process, as shown in Fig 1. This unique character of the water-jet guided laser provides a method of SCD machining.

The key parameters of the water-jet guided laser that affects cutting quality are nozzle diameter, laser power and cutting speed. SCD dimension decides which nozzle diameter is applied, and the bigger the nozzle diameter the deeper and larger of the cutting kerf. Cutting speed and laser power will be discussed in the following as the significant parameter effect on the cut quality. Therefore, it is important to understand how process parameter of water-jet guided lasers influence the slicing SCD compare to conventional dry-lasers.

This research was proceeding to probes relationship between laser power and cutting speeds in getting the best slicing result and outlines the effect of the laser cutting parameters on HAZ obtained in water-jet guided laser of the SCD sample. Several laser cutting parameters, for instance, laser power, cutting speed, height and nozzle size were considered influencing cutting result. The relationship between processing parameters and SCD sample slicing result in terms of optimum cutting conditions and the best kerf surface quality was observed via scanning electronic microscope (SEM). After slicing by both laser systems, the resulted samples were characterized by Raman spectroscopy respectively revealing cutting kerf surface residue.

2. Experimental

The micro-jet water guided laser system was developed by Dr. Bernold Richerzhagen of brand SYNOVA in type LCS150, which contained a Nd:YAG (Neodymium Doped Yttrium Aluminum Garnet) laser, and a 50 W high-power supply. The wavelength of the laser was 532 nm and the focusing system consisted of a quartz optical lenses, the pulse width was 1.12 ns, and pulse frequency was 6 kHz. The work piece is removable through X-axis, Y-axis and Z-axis. The micro water-jet was ultra-pure then went to high pressure pump system, which the adjustable nozzle flow pressure was set in 400 bar. The nozzle diameter was applied 30 um and helium gas was used in 1.1 L/min as protect gas.

The HPHT (001), single crystal artificial diamond substrate, in the dimension of 3×3×1 mm^3 was used in this research to be sliced. All the samples were identical and characterized by X-ray diffraction (XRD). All of samples were machined constantly at 25 mm from nozzle because of the laser produce nonlinear stimulated Raman scattering when water-jet is far away from material [11]. The experiment trials were conducted in random order to avoid any systematic errors and laser power intensity over cross section remained the same. The substrate treated by micro water-jet laser system and its working principle are shown in Fig. 1.

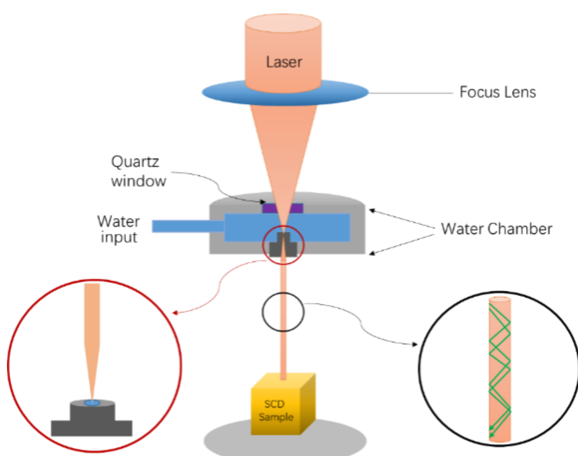

Fig. 1. Schematic of water-jet guided laser working principle (color online)

As comparison, conventional dry-laser (SMD rays, India) was applied. The laser source for this equipment was Nd:YAG in 1064 nm wavelength, and beam mode was 10W-TEM_{00}QS. For each comparison experiment, the working distance, laser power and scanning speed of laser maintains the same as micro water-jet guided laser.

Due to the high temperature of laser machining, a layer of non-diamond carbide that called Heat-affected zone (HAZ) has left from thermal process indicating the surface quality of machining, the less the HAZ the better the microstructure of the surface material that affects the performance of electron devices and an index for evaluation of the process technology. The quality of kerf feature and homogeneity for both laser systems were observed under SEM (ZEISS MERLIN Compact, Germany). The kerf surface after both laser system cutting were optically characterized by using the laser Raman microscope system (Horiba Scientific LabRAM HR Evolution, Kyoto, Japan) with 532-nm laser.

3. Results and discussions

In order to investigate the quality of SCD samples, XRD technique was applied at room temperature and the result is shown in Fig. 2, that FWHM value was 0.013° measured from the rocking curve. The proper controlling of the laser cutting process through appropriate selection of the cutting parameters is very important to achieve expected quality evaluation [12]. The cross sections of SCD samples under same laser power, cutting speed and height to work piece were 11 W, 8 mm/s and 25mm, respectively, of conventional dry-laser and water-jet guided laser system is shown in Fig. 3 (a)-(d) indicating diamond sacrifice and after-cutting quality. It is clearly seen that a graphite layer left on the surface of cutting kerf and a “V-shape” has turned out in cross section after dry-laser cutting, as shown in Fig 3 (a). The angle of “V-shape” kerf is calculated as 15.8° and the kerf width is 220.8 μm which was measured by SEM as shown in Fig. 3(b).

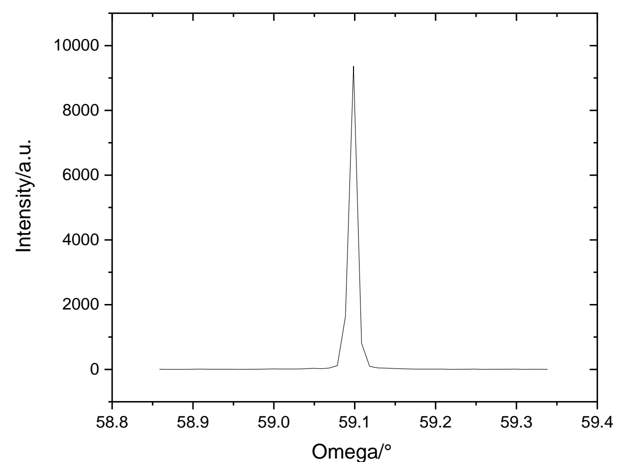

Fig. 2. XRD result of SCD sample

Micromorphology of kerf after conventional dry-laser SCD sample is rough with some cracks. For comparison, a linear kerf yielded a smooth and burr-free edge by using a water-jet guided laser is illustrated in Fig. 3(c), which was taken by optical microscope, and the 74.59 µm kerf width after cutting was measured by SEM as shown in Fig. 3(d). Therefore, the water-jet guided laser was chosen over conventional dry-laser for the rest of experiment because of its smaller material waste and better kerf surface quality, as well as, thin HAZ and kerf planeness result.

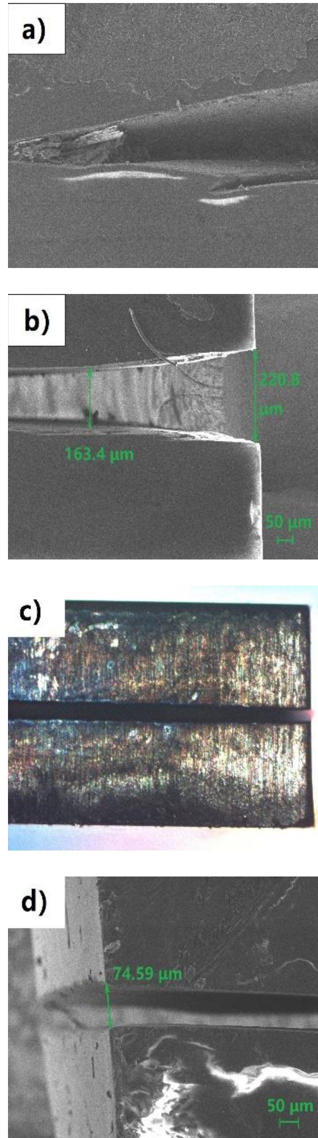

Fig. 3. Cross section images of SCD samples. Upper row: Cut quality of a commercial conventional dry-laser cutting machine. (a) after slicing a significant "V-shape" kerf of SEM image, (b) after slicing kerf width of SEM image. Lower row: Cut quality obtained by the water-jet guided laser. (c) after slicing kerf feature of optical microscope image, (d) after slicing kerf width of SEM image (color online)

To discover the best cutting parameters for 3x3x1 mm^3 SCD sample, laser power and cutting speed were assigned as variables respectively, and detailed data of water-jet guided laser were shown in Table 1(a) and (b). The height was maintained at a constant at 25 mm which was also deemed to be the accurate vertical distance to keep the stream from being broken. It was measured that laser power does degrade much within a stable length but a large amount of laser power decreased in a larger length region. The depths under various cutting speeds and laser power were measured by optical microscope (OM) showing a significant "shift" phenomenon.

Table 1. (a) Cutting parameters in constant speed and height, (b) Cutting parameters in constant laser power and height.

(a)

Sample#	Cutting Speed	Laser Power	Cutting Depth
	(mm/s)	(W)	(mm)
1	8	8	1.02
2	8	9	1.4
3	8	10	1.46
4	8	11	1.64(0.46, 0.84)

(b)

Sample#	Cutting Speed	Laser Power	Cutting Depth
	(mm/s)	(W)	(mm)
5	1	11	3
6	3	11	1.52 ~ 1.92 (0.21, 0.23)
4	8	11	1.64 (0.46, 0.84)
7	10	11	1.41 ~ 1.85 (0.11, 0.24)
8	20	11	1.4 (0.04, 0.13)

The SCD sample was set in constant height and cutting speed was 8 mm/s, laser power started to increasing from 8 W which is the minimum laser outlet power to cut SCD sample, as shown in Table 1(a). It is notable that the depth of the cutting increases with the increase of the power of the laser. When the laser power reaches 11.8 W, the SCD sample is completely sliced. Moreover, the output power of 11.8 W is within the safe use range of 13 W. When the laser powers were 8 W, 9 W and 10 W, the cutting depth were 1.02 mm, 1.40 mm, 1.46 mm, respectively. An increase in laser power could generate more heat on SCD kerf, which caused its temperature to rise to sublimation and fusion. Once laser power reached 11 W, the cutting depth increased to 1.64 mm and started to partially cut through. During that parameter, it had 0.46 mm and 0.84 mm width of two edges respectively, as marked parentheses in Table 1 and its SCD profile is illustrated in Fig. 4. The edge of SCD sample was cut deeper than the middle part because of draining water from kerf. Laser is introduced through a micro-thin high pressure water fiber. When the laser is working, the water can be easily removed from both ends of the trench at the

initial cutting stage. As the cutting continues, the trench gets deeper and water accumulates hindering the upcoming water and affecting the water discharge. Once some valleys formed in the bottom of trench, the water outlet gets even harder. Therefore, the laser beam scattered in condensed water and laser efficiency reduced. If one keeps increasing laser power to 11.8 W, SCD sample has been fully sliced. A full schematic diagram of SCD slicing processes are shown in Fig. 4.

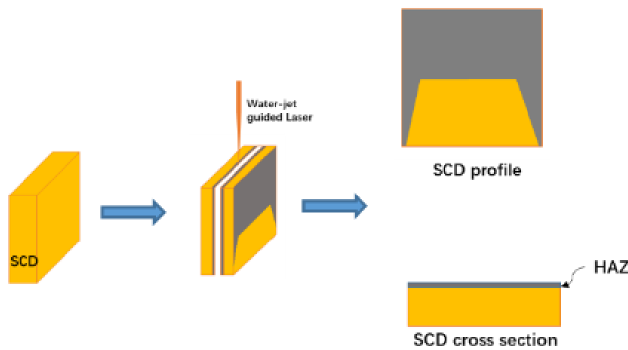

Fig. 4. Schematic diagram of SCD sample slicing process (color online)

Apart from laser power, cutting speed was tested as variable laser parameter for achieving best cutting technology result as shown in Table 1(b). The laser powers were constant at 11 W, due to the 13 W of safety working power and some cracks happened once laser power over 12 W, the tendency of cutting depth was decreased in general while cutting speed from 1 mm/s to 20 mm/s. When the cutting speed is 1 mm/s, SCD sample was sliced fully with a very rough kerf surface, then with the increasing cutting speed SCD sample just has two edges it cut thoroughly showing parentheses in Table 1. The reasonable explanation of this result is the heat accumulation effect of laser on the sample, the faster the cutting speed, the less thermal energy retains on the kerf surface. When the cutting speed was slow, a long time interaction between the laser beam and SCD sample happened and followed by a big amount of HAZ and cutting width. Fig. 5(a) shows that when the cutting speed is 1 mm/s, the #5 SCD sample was fully sliced with a visible rough kerf surface. In Fig. 5(b), the enlarged picture from OM indicates the roughness of kerf surface and some etching holes have appeared. Then the cutting speed increased to 3 mm/s, slice profile appeals a "M" shape which two edges (0.21 mm and 0.23 mm) cut thoroughly. If one keeps increasing the cutting speed to 8 mm/s, the fully cut part enlarged to 0.46 mm and 0.84 mm for two edges of the sample. Until it speeds up to 10 mm/s, the fully cut part shrank to 0.11 mm and 0.24 mm and the zig-zag section shown in the center as illustrated in Fig. 5(c)-(d). With prolonging cutting time, the zig-zag section will not be cut deeper because water hammer pressure is followed by the formula: $P = \frac{E(\nu \times \sin\theta)}{\omega}$ which E is the elastic modulus of water, ν is the initial velocity of water-jet leaving nozzle, θ is the angle of water-jet inflow and ω is the speed of sound in the jet [13].

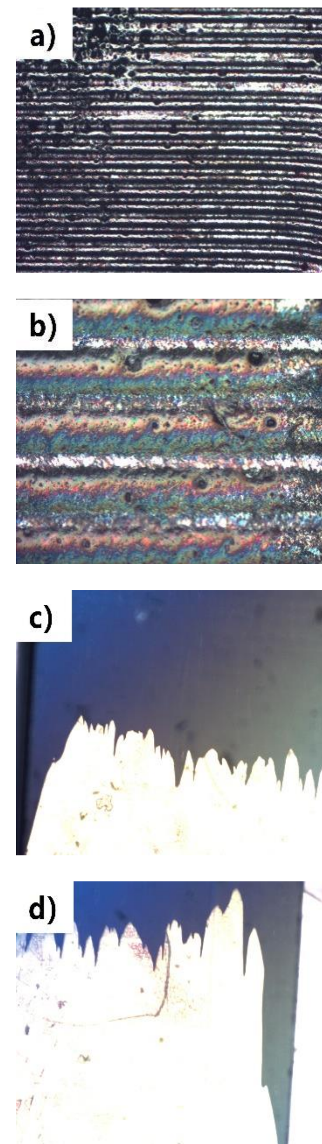

Fig. 5. Optical microscope images of sliced SCD samples. Upper row: Cutting speed of 1 mm/s, (a) kerf profile after sliced thoroughly, (b) enlarged picture of (a). Lower row: Cutting speed of 10 mm/s, (c)(d) zig-zag feature shown in the center (color online)

It is obtained that the angle of water-jet to the zig-zag peak is smaller than 90° indicating a smaller water pressure

than that to a flat surface. Thus, in the zig-zag section, the smaller the incident angle of the water-jet to zig-zag peak, the weaker SCD material to be damaged. The maximum speed tested in this research was 20 mm/s, the fully cut part kept shrinking (0.04 mm and 0.13 mm) and cut the depth lower to 1.4 mm as well, which was followed by an increase in cutting speed, the less heat than the SCD sample acquired from laser beams in the unit time. Therefore, among the SCD samples, which has list in Table 1 (a) and (b), the one under the parameters of 25mm working distance, 8 mm/s cutting speed and 11 W laser power indicating the best slicing result.

To quantify HAZ of SCD sample, Fig. 6 is a cross section SEM image of the sample under the chosen laser parameters. It is clearly seen that the kerf surface was flat and uniform, the thickness of HAZ was constant at 3.982 μm, which is thin enough for further polishing if needed. Therefore, this result indicating the laser parameter chosen for 3x3 SCD sample is good enough, because the higher laser power the enhanced HAZ and the faster cutting speed the lower HAZ [14]. The HAZ of that kerf surface was 3.982 μm illustrating a good quality as shown in Fig. 6(a). Hence, to obtain a fully sliced thin SCD, enhanced laser power of 11.8 W was needed and HAZ of 8.306 μm was measured by SEM as shown in Fig. 6(b).

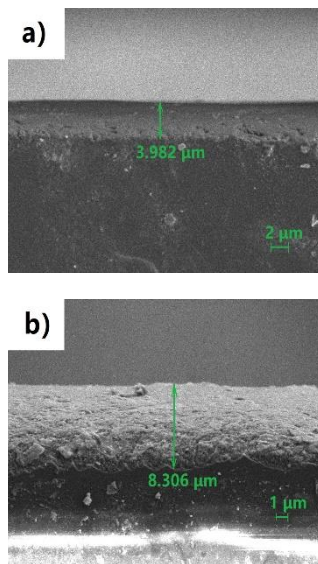

Fig. 6. Cross section SEM images in different laser power (a) 11W, (b) 11.8W. Cutting speed and height were 8 mm/s, 25 mm, respectively, for both SCD samples (color online)

Fig. 7 shows Raman spectroscopies of kerf surfaces of SCD samples after two laser system slicing respectively. Both Fig. 7(a) and (b) exhibit a Raman peak at 1332 cm^{-1}, which indicates good characteristic of diamond, and the related FWHM is 4.819 for after water-jet laser system sliced SCD as shown in Fig. 7(a). However, dry-laser SCD sample also shows a Raman peak at 1583 cm^{-1} revealing a first order spectrum of kish graphite and an additional disorder graphite peak at 1370 cm^{-1} overlapped with the pure diamond spectrum [15], as shown in Fig. 7(b). The results indicate that with the dry-laser system, a layer of graphite in the hexagonal plane carbon atoms structure was formed by the incoming intense laser energy from the diamond structure carbon atoms. It is noted that the same laser energy of both systems were able to melt diamonds into C atoms at 3823 K, due to the micro-jet water, the free state C atoms were not transferred to graphite.

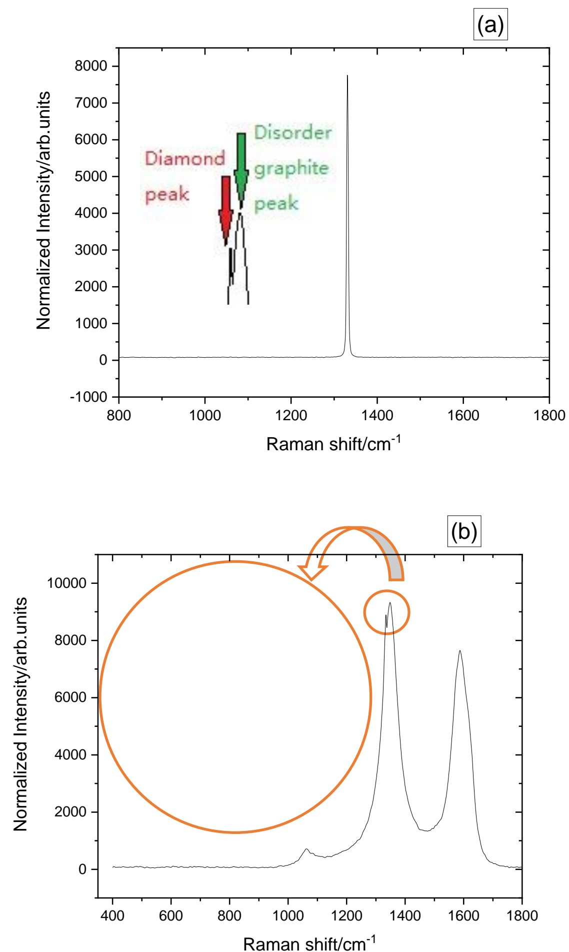

Fig. 7. Raman shift of resulted kerf surface in two laser system a) after water-jet guided laser, b) after conventional dry-laser and zoom-in overlapped spectra (color online)

4. Conclusions

In summary, the water-jet guided laser is a promising technology and has greater ability in cutting diamond area compared to conventional dry-laser slicing in material sacrifice and kerf feature. Based on the technical studies in parameter adjustment, this study found a suitable process of slicing SCD sample by using water-jet guided laser. The experimental results showed that the influence of laser power to cutting depth is linear growth, and the relationship of cutting speed and kerf quality is downward parabola

growth with increasing cutting speed. Apart from these two parameters, the water outlet is another factor affecting cutting depth, which both edges of sample werecut deeper than the middle part in general. Moreover, the dimension of 3x3x1 mm^3 SCD sample is fully sliced by water-jet guided laser system. The optimal cutting parameters of speed, laser power and height were 8 mm/s, 11.8 W, of 25 mm, respectively, and 8.306 μm of HAZ indicating a reasonable amount of material damage. The Raman spectroscopy was taken for both laser systems resulted kerf surfaces revealing only diamond characterized peak after water-jet guided lasers slicing, nevertheless, a significant graphite layer is formed after dry-laser system cutting.

Acknowledgements

This work was supported by the National Natural Science Foundation of China (No. 61804122, 61605155, 61627812, 61705176, and 11474048), the China Postdoctoral Science Foundation (No. 2019M653637 and 2019M660256) and Natural Science Fund of Shaanxi Province (No. 2018JQ6002).

References

[1] A. Caspi, Gem&gemology **33** (2), 102 (1997).
[2] K. Hirama, H. Sato, Y. Harada, H. Yamamoto, M. Kasu, IEEE Electron Device Lett. **33**(8), 1111 (2012).
[3] J. W. Liu, M. Y. Liao, M. Imura, H. Oosato, E. Watanabe, Y. Koide, Appl. Phys. Lett. **102**(11), 112910 (2013).
[4] T. Matsumoto, H. Kato, K. Oyama, T. Makino, M. Ogura, D. Takeuchi, T. Inokuma, N. Tokuda, Sci. Rep. **6**(1), 31585 (2016).
[5] K. Hirama, K. Tsuge, S. Sato, T. Tsuno, Appl. Phys. Express **3**(4) 044001 (2010).
[6] Y. Kitabayashi, T. Kudo, H. Tsuboi, T. Yamada, D. Xu, M. Shibata, D. Matsumura, Y. Hayashi, M. Syamsul, M. Inaba, A. Hiraiwa, H. Kawarada, IEEE Electrl. Device L **38**(3) 363 (2017).
[7] W. M. Steen, J. Opt. A Pure Appl. Opt. **5**(4), S3 (2003).
[8] Q. Liu, X. Duan, C. Peng, Novel Optical Technology for Nanofabrication, Springer, 1, 2014.
[9] J. Dutta Majumdar, I. Manna, Laser processing of materials. Sadhana-acad P Eng. S. **28**(3-4), 495 (2003).
[10] V. M. Tabie, M. O. Koranteng, A. Y. F. Kuuyine. Laser in manufacturing and material processing **6**, 189 (2019).
[11] T. Z. Kosc, K. L. Marshall, A. Trajkovska-Petkoska, R. Varshneya, S. D. Jacobsm Optics & Photonics News **15**(12), 33 (2004).
[12] B. S. Yilbas, M. M. Shaukat, F. Ashraf. Opt. Laser Technol. **93**(1), 67 (2017).
[13] X. Chen, X. Xu, W. Liu, L. Huang, H. Li, C. Wu et al., Materials **13**(14), 3206 (2020).
[14] I. Masumoto, T. Shinoda, H. Ishiyama, Japan Welding Soc. **3**(1), 126 (1985).
[15] S. Reich, C. Thomsen, Phil. Trans. R. Soc. Lond. A **362**, 2271 (2004).

*Corresponding author: hxwangcn@mail.xjtu.edu.cn